Published in final edited form as:
Twin Res Hum Genet. 2012 June ; 15(3): 336–350. doi:10.1017/thg.2012.14.

White Matter Heritability Using Diffusion Tensor Imaging in Neonatal Brains

Xiujuan Geng[1], **Elizabeth C. Prom-Wormley**[5], **Javier Perez**[5], **Thomas Kubarych**[5], **Martin Styner**[1,2], **Weili Lin**[3,4], **Michael C. Neale**[5], and **John H. Gilmore**[1]

[1]Department of Psychiatry, University of North Carolina-Chapel Hill, Chapel Hill, USA

[2]Department of Computer Science, University of North Carolina-Chapel Hill, Chapel Hill, USA

[3]Department of Radiology, University of North Carolina-Chapel Hill, Chapel Hill, USA

[4]Biomedical Research Imaging Center, University of North Carolina-Chapel Hill, Chapel Hill, USA

[5]Virginia Institute for Psychiatric and Behavioral Genetics, Virginia Commonwealth University, Richmond, USA

Abstract

Understanding genetic and environmental effects on white matter development in the first years of life is of great interest, as it provides insights into the etiology of neurodevelopmental disorders. In this study, the genetic and environmental effects on white matter were estimated using data from 173 neonatal twin subjects. Diffusion tensor imaging scans were acquired around 40 days after birth and were non-rigidly registered to a group-specific atlas and parcellated into 98 ROIs. A model of additive genetic, and common and specific environmental variance components was used to estimate overall and regional genetic and environmental contributions to diffusion parameters of fractional anisotropy, radial diffusivity, and axial diffusivity. Correlations between the regional heritability values and diffusion parameters were also examined. Results indicate that individual differences in overall white matter microstructure, represented by the average diffusion parameters over the whole brain, are heritable, and estimates are higher than found in studies in adults. Estimates of genetic and environmental variance components vary considerably across different white matter regions. Significant positive correlations between radial diffusivity heritability and radial diffusivity values are consistent with regional genetic variation being modulated by maturation status in the neonatal brain: the more mature the region is, the less genetic variation it shows. Common environmental effects are present in a few regions that tend to be characterized by low radial diffusivity. Results from the joint diffusion parameter analysis suggest that multivariate modeling approaches might be promising to better estimate maturation status and its relationship with genetic and environmental effects.

Keywords

heritability; genetic variation; environmental variation; magnetic resonance imaging (MRI); diffusion tensor imaging (DTI); white matter maturation; white matter atlas; neonates; fractional anisotropy; radial diffusivity; axial diffusivity

ADDRESS FOR CORRESPONDENCE: Dr. Xiujuan Geng, Department of Psychiatry, 229 Medical School Wing B, University of North Carolina, Chapel Hill, NC 27514, USA. xiujuangeng@med.unc.edu.

Twin studies provide important insights into the genetic basis of phenotypic variation of the human brain. Studies of adult twins show that genes play a significant role in the variability of global brain volumes, including total intracranial, total gray matter (GM), and white matter (WM) volumes (Peper et al., 2007; Posthuma et al., 2000; Schmitt et al., 2007), and local regional gray and white volumes (Hulshoff Pol et al., 2006; Thompson et al., 2001). Other brain measures, such as cortical thickness and surface area, are also highly heritable in adults (Panizzon et al., 2009; Schmitt et al., 2008). Not only structure, but also the 'default-mode' network (Glahn et al., 2010) and cognitive function, such as working memory (Blokland et al., 2011; Karlsgodt et al., 2010; Koten et al., 2009), have been shown to relate to genetic factors using functional magnetic resonance imaging (fMRI). A few studies suggest that global and regional GM and WM structures (Peper et al., 2009) and cortical networks (Schmitt et al., 2008) are also heritable in pediatric populations.

Little is known about genetic and environmental contributions to human brain development in the early years of life. The first years of life involve the most dynamic growth of brain structure and function during postnatal development (Gilmore et al., 2007, Knickmeyer et al., 2008). The degree to which genes and environment generate individual differences in early brain development is of fundamental importance in understanding developmental trajectories during childhood, and may help the early identification and prevention of various neurodevelopmental disorders (Gilmore et al., 2010; Schmitt et al., 2007). Our previous study in neonatal twins (Gilmore et al., 2010) revealed that the heritabilities of total intracranial volume (.73) and total WM volume (.85) were high, and similar to those reported in older children and adults, while GM volume heritability was lower (.56). However, it is not clear whether variation in WM microstructure, such as fiber organization and myelination, is under genetic or environmental control in early childhood.

WM maturation is a complex and lengthy process; the most significant period of myelination occurs between midgestation and the second postnatal year (Brody et al., 1987; Yakovlev and Lecours, 1967). DTI enables non-invasive estimation of WM microstructure and pathways by measuring water diffusion properties in brain tissues (Basser et al., 1994; Le Bihan et al., 2001). DTI-extracted parameters, such as apparent diffusion coefficients, including radial diffusivity (RD), axial diffusivity (AD), and fractional anisotropy (FA), are possible indicators of axonal organization, density, and degree of myelination (Beaulieu, 2002; Neil et al., 1998; Song et al., 2002). RD and AD describe the diffusion degree perpendicular to and parallel to fiber tracts, respectively, and the normalized parameter FA estimates the anisotropy degree of the diffusion process. DTI studies in adult twins have reported high heritability in the microstructure of the splenium and genu corpus callosum (Pfefferbaum et al., 2001), and of FA in bilateral frontal, parietal and left occipital lobes (Chiang et al., 2009). It has been shown that the whole brain WM FA and RD show significant genetic variability, with heritability values of .52 and .37, respectively (Kochunov et al., 2010). Genetic variation in AD was nonsignificant in that study, and estimates of heritability vary among different major fiber regions. A recent WM developmental study of persons aged 12 to 29 years indicated genetic variation in WM integrity (represented by FA), and that the effects vary with age (higher in adolescence than adulthood), gender, socioeconomic status, and IQ (Chiang et al., 2011). A study in nine-year-old children reported that RD and AD, rather than FA, were significantly influenced by genetic factors (Brouwer et al., 2010). Additional studies of larger samples are needed to clarify the pattern of results across ages, tracts, and DTI measures.

The aim of the present study was to assess the early genetic and environmental influences on the WM microstructure in neonates. We hypothesized that WM is highly heritable, that genetic influences vary in different brain regions, and that the non-uniformity in each individual might be related to the maturation pattern. Due to the inconsistent previous

findings of genetic effects on different diffusion measures, the three commonly used parameters FA, RD, and AD, were analyzed in this study. Structural equation modeling was used to estimate global and regional genetic and environmental effects in a sample of neonatal twin pairs. It has been suggested that the diffusion measures are associated with WM development (Dubois et al., 2006, Gao et al., 2009). During the maturation process, decreases in RD may reflect axonal myelin synthesis and proliferation of glial cells. Increases in FA could reflect fiber organization, and may also be attributed to decreases in RD (Partridge et al., 2004). Therefore the correlation between heritability estimates and the level of RD were computed to explore whether regional genetic variation is modulated by the maturation degree in the first few months of life.

Methods

Subjects

The Institutional Review Board of the University of North Carolina (UNC) School of Medicine and Duke University Medical Center (DUMC)approved this study. Mothers with same-sex twin pregnancies were recruited from the outpatient OB-GYN clinics at UNC Hospitals and DUMC. Exclusion criteria included maternal HIV infection, major congenital abnormality on fetal ultrasound, and chromosomal abnormalities of fetuses. Informed consent was obtained from the parents of all subjects. For zygosity testing, polymerase chain reaction–short tandem repeat (PCR–STR) analysis of 14 loci was performed on DNA isolated from buccal swab cell collection (BRT Laboratories, Baltimore, MD). The study sample consisted of 173 individual participants comprising 63 complete same-sex twin pairs — 31 monozygotic (MZ) and 32 dizygotic (DZ) — and 47 unpaired twins. Two twin pairs from a single mother are included, though treated as independent pairs in the statistical analysis. Demographic and clinical variables are presented in Table I.

Image Acquisition and DTI Preprocessing

All neonatal MRI scans were acquired on a head-only 3T scanner (Allegra, Siemens Medical Solutions, Erlangen, Germany) around 40 postnatal days of age (see Table 1). All subjects were scanned without sedation. Before neonates were imaged, they were fed, swaddled, and fitted with ear protection. Once asleep they were fitted with earplugs or earphones and placed in the MRI scanner with head in a vacuum-fixation device. Scans were performed with a neonatal nurse present, and a pulse oximeter to monitor heart rate and oxygen saturation. A single-shot echo-planar spin echo DTI sequence was used with the following variables: TR 5,200 ms, TE = 73 ms, slice thickness = 2 mm, in-plane resolution = 2×2 mm^2, and 45 slices. One image without diffusion gradients (b = 0) and diffusion-weighted images (DWIs) along 6 gradient directions, with a b value of 1,000 mm^2/sec, were acquired. The acquisition was repeated five times to improve signal-to-noise ratio. DWIs were screened offline for motion artifacts and for missing and corrupted sections using an automatic DWI quality control tool, DTIPrep (http://www.nitrc.org/projects/dtiprep). Diffusion images with large motion artifacts were excluded from the entire set of DWIs. The DWIs with more than 70% successful rate were retained for later analysis. After the offline screening, the five repeated sequences were combined into a single DWI volume and the diffusion maps, such as RD, AD, and FA, were then estimated using standard weighted least square fitting (Liu et al., 2010).

DTI Registration and White Matter Parcellation

All tensor images (173 in total) were first rigidly aligned and the average computed and used as the initial template. The original DTI data was affine-aligned to it, and a new average tensor image was computed for the updated template, which is sharper than the initial one. Affine registration was repeated three times; little change was found between the average

images from the third and second iteration, indicating that the initial template converged after the third iteration. The affine-aligned tensors were then mapped to an iteratively updated group average with an unbiased group-wise tensor-based deformable registration method (Zhang et al., 2007). At each iteration, all input images were warped to the average of the registered tensors in the previous iteration. This deformable registration was repeated six times, allowing the convergence of the group average, that is, the template. The tensor-based rigid, affine, and non-rigid registrations were performed using a publicly available toolkit, DTITK (http://dtitk.sourceforge.net/pmwiki/pmwiki.php). The RD, AD, and FA maps (Figure 1) were then warped to the template space using their corresponding affine matrices and deformation fields estimated from the above registration process.

We adapted the recently developed WM atlas JHU-DTISS (a.k.a. 'Eve atlas', http://lbam.med.jhmi.edu/) (Oishi et al., 2009), to obtain a comprehensive WM parcellation for calculation of regional average diffusion parameters. The FA map of the atlas was affine-aligned and then deformably registered to the average FA maps of our warped neonatal DTI data. The 'Type II' WM parcellation with 130 labels was mapped to the neonatal space following the affine and non-rigid transformations with nearest neighbor interpolation. This parcellation included 52 gyri regions (including 44 superficial WM regions), 56 deep WM regions, 10 subcortical regions, and 12 other regions. The boundary of the cortex and WM of our DTI atlas was defined by an FA threshold of .1. Since most WM regions are not myelinated at birth, the FA values are lower compared to those in adults (Dubois et al., 2008). The boundary was used to define the superficial WM regions included in the corresponding gyri from the Type II parcellation. In this study, we included 44 superficial WM ROIs, 52 deep WM ROIs (bilateral inferior cerebral peduncle and medial lemniscus were excluded due to the very small coverage of the ROIs with less than 10 voxels in the neonatal atlas), and bilateral cerebellum WM, 98 WM ROIs in total. The abbreviations of each ROI can be found in the Appendix. For every registered individual diffusion map, the FA, RD, and AD were averaged over each ROI. Therefore, the three sets of 98 diffusion parameters from each subject were obtained (see Figure 2(a)) and ready for the following statistical analyses.

Estimation of Genetic and Environmental Effects

Genetic and environmental variation in the average whole brain (thresholded with FA > .1), left and right hemispheres, and ROI measures of WM integrity (FA, AD, and RD) were estimated using a classic univariate twin modeling approach (Neale & Cardon, 1992). This approach utilizes MZ and DZ twin pair variances and covariances to estimate the proportion of total phenotypic variance due to additive genetic, shared environmental, and unique environmental influences. Additive genetic effects (A) refer to the additive effects of alleles at every locus; shared environmental effects (C) are those effects shared by twin pairs; and unique environment effects (E) refer to effects not shared by twin pairs and include measurement error. Univariate analysis parameterizes the total phenotypic variance as $\sigma^2_V = \sigma^2_A + \sigma^2_C + \sigma^2_E$. Twin covariances are parameterized as $\sigma^2_{covMZ} = \sigma^2_A + \sigma^2_C$ and $\sigma^2_{covDZ} = .5\sigma^2_A + \sigma^2_C$. The full ACE model and its submodels, (i.e. AE, CE, and E only) were fitted to test the significance of additive genetic and shared environmental effects on the three sets of imaging measures. Model fitting used maximum likelihood (Edwards, 1984) by calculating twice the negative log-likelihood of the raw data for each twin pair, and summing across all pairs. Because the variance component estimates are zero-bounded, the difference between an original model and its respective submodels follows a 50:50 mixture of zero, and a χ^2 distribution with degrees of freedom equal to the difference in model parameters ($df = 1$ for AE and CE models, $df = 2$ for an E-only model).

There were significant ($p < .05$) associations between diffusion measures and gestational age at MRI in most ROIs. Similarly, significant differences in mean intensity ($p < .05$) were

detected by gender in approximately 5% of all positions. All analyses included sex and the linear effects of gestational age at the MRI scan as fixed effects in the means models. Prior to ACE submodel comparisons, saturated models were fitted to test for group differences in mean and variances, and to estimate cross-twin correlations by zygosity. Maximum likelihood analyses of individual observations were used for all analyses as implemented in OpenMx 1.1, a package for use within the R language (Boker et al., 2011).

Analysis of Relationship Between Heritability and Diffusion Measures

Mean FA, RD, and AD were calculated across the whole population over each ROI. Three linear regression analyses were performed on the mean FA and FA heritability, mean RD and RD heritability, and mean AD and AD heritability separately.

A single parameter may not be specific to maturation status. High FA might not indicate high maturation (e.g., splenium and genu of the corpus callosum have high FA values after birth, but are not myelinated until later years of age). In general, a high RD region where fibers follow similar directions might indicate a low myelination degree. However, regions with more complex fiber organization, such as crossing fibers, may also appear to have high RD, despite being highly myelinated. Since RD rather than AD has been shown to be better representative of changes in demyelination models (Song et al., 2003), we analyzed the data by considering both FA and RD. The ROIs were separated into four subgroups according to high/low FA (20 ROIs with the highest/lowest FA) and high/low RD (20 ROIs with the highest/lowest RD) values, and the genetic effects were summarized under the four conditions: HL, HH, LL and LH (see Table 3). HL (high FA and low RD) might be associated with high maturation; HH indicates regions that are well organized but have low maturation; LL may correspond to high maturation regions with complex fiber organization; and LH might represent a low degree of maturation.

Results

Both qualitative and quantitative tests suggested that the population distribution of most ROIs approximated a normal distribution. Similarly, there were no statistically significant differences in means and variances between MZ and DZ twins for most structures. Population means and variances are reported in Table 4.

Global Analysis

There was significant heritability across all three average diffusion parameters over whole brain WM (Table 2). FA had the highest heritability, .60, 95% CI [.22, .91], followed by AD, .57, 95% CI [.19, .90], and RD, .53, 95% CI [.19, .91]. There was significant heritability in both hemispheres of FA: left, .56, 95% CI [.16, .89], right, .60, 95% CI [.20, .90]; and RD: left, .45, 95% CI [.09, .88], right, .60, 95% CI [.27, .93]. AD heritability was significant in the right hemisphere only, .68, 95% CI [.30, .92].

Regional Analysis

The regional diffusion parameters of each ROI are listed in Table 4. The mean FA values range from .11 to .38; D varies within $0.79 \sim 1.65 \times 10^{-3}$ mm^2s^{-1}, and AD varies between $1.09 \sim 2.17 \times 10^{-3}$ mm^2s^{-1}. Posterior limb of internal capsule (PLIC), retrolenticular part of internal capsule (RLIC), and the splenium and genu of the corpus callosum show larger FA values. PLIC, pontine crossing tracts, corticospinal tracts, midbrain, anterior limb of internal capsule (ALIC), and RLIC have smaller RD than other regions. These findings are consistent with our previous early WM developmental study focused on the major fiber bundles (Geng et al., 2011). Superficially located WM in cortical regions has lower FA values compared to deep WM.

Among the majority of ROIs, MZ twin pairs had increased correlations of FA, RD, and AD compared with DZ twin pairs, suggesting significant additive genetic effects. In general, heritability shows heterogeneity over WM tissue (Figure 2b). There are about half of the ROIs with high heritability (A > .50, $p < .05$) on RD (49 ROIs), AD (42 ROIs), and FA (42 ROIs) measures. Many fewer ROIs show high common environment effects (C > .50, $p < .05$) for RD (10 ROIs), AD (7 ROIs) and FA (3 ROIs) (Table 4).

For FA heritability, left posterior corona radiata shows the highest genetic variation (A = .82). There are seven regions with relatively high RD heritability estimates with A > .80: superficial WM regions in left middle and inferior occipital gyrus, right pre-cuneus, and right inferior temporal gyrus, and deep WM regions of right sagittal stratum, right splenium of corpus callosum, and left posterior corona radiata. The corresponding RD values in these regions are relatively high (between 1.19 and 1.30).

For AD heritability, right posterior corona radiata show the highest genetic variation with A=.92. For the estimates of environmental variation, WM in the left inferior temporal gyrus has the highest FA environmental variation with C = .69. Bilateral external capsule and left PLIC have relatively high RD environmental variation with C > .7, and right external capsule shows the highest value of C = .82. Left external capsule and WM in left angular gyrus show the highest environmental variation of AD with C = .71.

Relationships Between Heritability and Diffusion Measures

There is no correlation between FA heritability and mean FA throughout the 98 ROIs (Figure 3). There is a significant positive correlation between RD heritability and mean RD ($r = .17$, $p < 10^{-5}$), and a significant positive correlation between AD heritability and mean AD ($r = .05$, $p = .02$).

Genetic variation in FA and RD under the four conditions, HL, HH, LL, and LH, is described in Table 3. We note that ROIs with high FA and low RD include major projection fibers with known earlier maturation after birth (Kinney et al., 1988). All these regions show low genetic effect on FA, and most of these regions show low genetic effect on RD (except for right RLIC and right superior cerebral peduncle). ROIs with high FA and high RD include bilateral body corpus callosum, right posterior thalamic radiation, and left tapetum. All these regions have high FA heritability, and all but left tapetum has high RD heritability. ROIs with low FA and low RD include bilateral cerebellum with high RD and FA heritability. ROIs with low FA and high RD include a few superficial WM regions in bilateral lingual gyrus, bilateral middle frontal orbital gyrus, and right lateral frontal orbital gyrus.

Discussion

Genetic Effects Related to Overall White Matter Microstructure

This is the first twin study to assess the genetic and environmental contributions to WM microstructure measured by DTI in neonates. The heritability estimates for DTI measures averaged over the whole brain WM (FA = .60, RD = .53, and AD = .57) were higher than those reported for an adult population (FA = .52, RD = .37). Further, no significant genetic effects were detected for AD in the adult study (Kochunov et al., 2010). WM development is a complex process that continues into adulthood. During the long maturation process, different environmental exposures likely play a role in neuronal plasticity and influence the WM integrity of individuals (Bengtsson et al., 2005). Therefore, genetic variation might decrease with development and aging. The higher heritability estimates for diffusion measures, especially for RD and AD (for RD, $A_{Left} = .45$, $A_{Right} = .60$; for AD, $A_{Left} = .43$,

A_{Right} = .68), may correspond to WM microstructure asymmetries in adults (Jahanshad et al., 2010), and to brain structural asymmetries that appear in neonates (Gilmore et al., 2007).

Heterogeneous Heritability Across Regions of Interest

Results from regional ACE analysis indicate that the magnitude of genetic effects differs across WM regions. About half of the regions analyzed show high heritability in the diffusion measures. Among RD measures, the regions with the largest magnitude of heritability include left middle (.86) and left inferior occipital WM (.84), right inferior temporal (.84), and right pre-cuneus WM, part of the superior parietal lobule (.84). There was no significant genetic contribution for several major WM fiber bundles, such as bilateral uncinate fasciculus RD. Interestingly, the WM regions with the highest RD heritability have low FA heritability (A = .23–.48), whereas the uncinate fasciculus shows relatively high FA heritability (left/right: .62/.58).

The inconsistent genetic effects on RD and FA over several WM regions suggest that these two measures reflect distinct WM biological properties that are shaped differently by genetic and environmental effects. Future multivariate approaches focusing on the shared genetic and environmental effects between these measures could help elucidate this relationship.

Substantial Shared Environmental Effects in Specific Regions of Interest

Bilateral PLIC, ALIC, external capsule, uncinate fasciculus, and left middle cerebellar peduncle show high shared environmental effects in RD ranging from .57 to .82. The AD of bilateral external capsule, middle cerebellar peduncle, and inferior frontal occipital fasciculus also has a large proportion of shared environmental effects, ranging between .47 and .71. Shared environmental effects are substantial for the RD measure of bilateral external capsule (left/right: .73/.82). Located between the putamen and claustrum, and lateral to the internal capsule, the external capsule is believed to contain association fibers, such as the superior longitudinal fasciculus, inferior frontal occipital fasciculus, and commissural fibers, and is not devoid of projection fibers. Together with PLIC and ALIC, the external capsule may have started myelination earlier prenatally than other association fibers (Kinney et al., 1988). Prenatal neurohormonal and uterine environment could affect the maturation process, which might lead to pronounced shared environmental variation in the maturation process. The significant genetic contributions in these regions observed in adults (Kochunov et al., 2010) may indicate the canalization effect (Gilmore et al., 2010; Lenroot & Giedd, 2008). For example, cumulative genetic effects determine the endpoint of development, while early trajectories of development may be influenced more by environmental factors.

Relationships Between Genetic Variation and Maturation Status

The significant correlations between heritability and the mean diffusion levels of RD and AD suggest that genetic variation in WM microstructure may be modulated by maturation status in neonates. Membrane proliferation, one major WM maturation process, would lead to decreased RD and AD, and unchanged FA; fiber myelination, another major maturation process, would correspond to decreased RD, increased FA, and unchanged AD (Dubois et al., 2008). Studies in animal models that manipulate cerebral myelination levels showed that RD is highly sensitive to regional demyelination (Song et al., 2003). Infant WM development studies (Gao et al., 2009, Geng et al., 2011) observed significant increases in FA and significant reductions in RD and AD during the development of the first years of life. The positive correlation (r = .17, p < .00001) between RD heritability estimates and mean levels of RD suggests that fibers with higher maturation in neonates are possibly influenced more by prenatal common or unique environmental factors.

There was no significant association between estimates of heritability for FA and the average FA value across all ROIs. Fibers with higher FA values may not necessarily correspond to higher maturation degree in terms of myelination compared to other fibers at the same time point. Dense well-organized fibers (e.g., corpus callosum) may present high FA values when unmyelinated. Measures taking into account complex fiber structures based on high angular resolution diffusion imaging techniques may better reflect fiber maturation. With the current data acquisition limitation, joint analysis of FA and RD may reflect the maturation status better than univariate analyses of each measure. After separating the WM into four groups, based on high and low mean values of FA and RD, we noticed that major projection fibers fall in the HL group, consistent with previous infant WM maturation studies (Dubois et al., 2006; Yakovlev & Lecours, 1967). These projection fibers show low heritability estimates of RD and FA in general. Cerebellum is in the LL group with high genetic effect. The HH group includes the corpus callosum and thalamocortical fibers, which are less mature than the HL group and show high heritability estimates. The LH group contains several superficial WM regions with higher genetic control compared to the HL group. These analyses show a promising beginning to the study of genetic and environmental variation in neuronal maturation.

It is possible that differences in heritability across regions could be driven by changes in the reliability of the measures. The reliability of the measures is likely to be higher in regions with higher FA values. If differences in heritability were driven by the reliability of the measures, a positive correlation, rather than no correlation, would be detected between FA and FA heritability. It is also possible that the sample size of this study may be insufficient to detect significant additive genetic effects, which may explain the lack of significant heritability for some measures. Clarification of these issues is expected to be addressed as sample size increases over time and as longitudinal data become available in our ongoing longitudinal study.

We adapted a recently developed WM atlas for singletons with 130 ROIs to parcellate our neonatal DTI images automatically in twins. WM differences between non-twins and twins may be apparent, especially among neonates. Subsequently, we warped the twin atlas used in this study together with the ROIs to our population-specific atlas, which is expected to reduce any effect caused by using the non-twin atlas. Compared to tractography-based approaches, which may only focus on major or more visible fiber tracts, our approach has a wider coverage of the WM. Due to the relatively low signal-to-noise ratio of the neonatal data (smaller brain size and shorter scanning time constrained by the baby's sleeping time), the voxel-based DTI analysis used by several DTI heritability studies in pediatric and adult groups may prove difficult to apply to neonatal brain image data. The ROI-based average regional measure used here is one way to overcome this limitation, as it decreases spatial resolution to increase data reliability. Future efforts to optimize the neonatal DTI atlas are expected to decrease measurement variability.

While there were significant mean differences for ROIs by gender, specific models testing the contribution of sex to the etiology of WM development could not be tested due to the absence of opposite-sex DZ twin pairs. Consequently, these results cannot resolve questions of genetic and environmental heterogeneity by gender in the development of WM. Nevertheless, these results provide comprehensive insight into the genetic and environmental contributions to WM during early human development.

The statistical tests of the genetic and environmental components (shown in Table 4) were not corrected for multiple comparisons. In the present context we do not seek to establish the statistical significance of the most heritable region, which would be analogous to, for example, correcting the *p*-value of the most significant SNP association in a genome-wide

association study. Instead we wish to report the parameter estimates across a large number of different regions. A Q-Q plot would show that there is ample evidence of departure from the expectation under the null hypothesis that none of the regions demonstrates statistically significant heritability.

Conclusion

We have conducted the first twin study of neonatal brain WM microstructure with DTI. In general, substantial heritability of the average DTI parameters was found over the whole-brain WM and is higher than that which has been reported for adults. Genetic and environmental effects are heterogeneous and display a wide range in magnitude over different WM regions. Significant positive correlation between heritability and diffusion measures suggests that regional genetic effects may be modulated by maturation status of the neonatal brain—the more mature the region, the less heritable its variation. Common environmental effects are present in fewer regions that tend to be characterized by low RD. Our joint diffusion parameter analysis suggests that multivariate modeling approaches that jointly analyze the diffusion parameters are promising approaches to estimating maturation status and its relationship with genetic and environmental effects.

Acknowledgments

This work was supported by the National Institutes of Health grants MH070890 (J. H. Gilmore), MH-65322 (M. C. Neale), and NIMH Training Grant MH-20030.

References

Basser PJ, Mattiello J, Le Bihan D. MR diffusion tensor spectroscopy and imaging. Biophysical Journal. 1994; 66:259–267. [PubMed: 8130344]

Beaulieu C. The basis of anisotropic water diffusion in the nervous system — a technical review. NMR in Biomedicine. 2002; 15:435–455. [PubMed: 12489094]

Bengtsson SL, Nagy Z, Skare S, Forsman L, Forssberg H, Ullen F. Extensive piano practicing has regionally specific effects on white matter development. Nature Neuroscience. 2005; 8:1148–1150.

Blokland GA, McMahon KL, Thompson PM, Martin NG, de Zubicaray GI, Wright MJ. Heritability of working memory brain activation. Journal of Neuroscience. 2011; 31:10882–10890. [PubMed: 21795540]

Boker S, Neale M, Maes H, Wilde M, Spiegel M, Brick T, Spies J, Estarbrook R, Kenny S, Bates T, Mehta P, Fox J. OpenMx, An open source extended structural equation modeling framework. Psychometrika. 2011; 76:306–317. [PubMed: 23258944]

Brody BA, Kinney HC, Kloman AS, Gilles FH. Sequence of central nervous system myelination in human infancy. I An autopsy study of myelination. Journal of Neuropathology and Experimental Neurology. 1987; 46:283–301. [PubMed: 3559630]

Brouwer RM, Mandl RC, Peper JS, van Baal GC, Kahn RS, Boomsma DI, Hulshoff Pol HE. Heritability of DTI and MTR in nine-year-old children. Neuroimage. 2010; 53:1085–1092. [PubMed: 20298793]

Chiang MC, Barysheva M, Shattuck DW, Lee AD, Madsen SK, Avedissian C, Klunder AD, Toga AW, McMahon KL, de Zubicaray GI, Wright MJ, Srivastava A, Balov N, Thompson PM. Genetics of brain fiber architecture and intellectual performance. Journal of Neuroscience. 2009; 29:2212–2224. [PubMed: 19228974]

Chiang MC, McMahon KL, de Zubicaray GI, Martin NG, Hickie I, Toga AW, Wright MJ, Thompson PM. Genetics of white matter development: A DTI study of 705 twins and their siblings aged 12 to 29. Neuroimage. 2011; 54:2308–2317. [PubMed: 20950689]

Dubois J, Dehaene-Lambertz G, Perrin M, Mangin JF, Cointepas Y, Duchesnay E, Le Bihan D, Hertz-Pannier L. Asynchrony of the early maturation of white matter bundles in healthy infants:

Quantitative landmarks revealed noninvasively by diffusion tensor imaging. Human Brain Mapping. 2008; 29:14–27. [PubMed: 17318834]

Dubois J, Hertz-Pannier L, Dehaene-Lambertz G, Cointepas Y, Le Bihan D. Assessment of the early organization and maturation of infants' cerebral white matter fiber bundles: A feasibility study using quantitative diffusion tensor imaging and tractography. Neuroimage. 2006; 30:1121–1132. [PubMed: 16413790]

Edwards, AWF. Likelihood. Cambridge: Cambridge University Press; 1984.

Gao W, Lin W, Chen Y, Gerig G, Smith JK, Jewells V, Gilmore JH. Temporal and spatial development of axonal maturation and myelination of white matter in the developing brain. American Journal of Neuroradiology. 2009; 30:290–296. [PubMed: 19001533]

Geng X, Gouttard S, Sharma A, Gu H, Styner M, Lin W, Gerig G, Gilmore JH. Quantitative tract-based white matter development from birth to age two years. Neuroimage. 2012; 61:542–557. [PubMed: 22510254]

Gilmore JH, Lin W, Prastawa MW, Looney CB, Vetsa YS, Knickmeyer RC, Evans DD, Smith JK, Hamer RM, Lieberman JA, Gerig G. Regional gray matter growth, sexual dimorphism, and cerebral asymmetry in the neonatal brain. Journal of Neuroscience. 2007; 27:1255–1260. [PubMed: 17287499]

Gilmore JH, Schmitt JE, Knickmeyer RC, Smith JK, Lin W, Styner M, Gerig G, Neale MC. Genetic and environmental contributions to neonatal brain structure: A twin study. 2010; 31:1174–1182.

Glahn DC, Winkler AM, Kochunov P, Almasy L, Duggirala R, Carless MA, Curran JC, Olvera RL, Laird AR, Smith SM, Beckmann CF, Fox PT, Blangero J. Genetic control over the resting brain. Proceedings of the National Academy of Sciences USA. 2010; 107:1223–1228.

Hulshoff Pol HE, Schnack HG, Posthuma D, Mandl RC, Baare WF, van Oel C, van Haren NE, Collins DL, Evans AC, Amunts K, Burgel U, Zilles K, de Geus E, Boomsma DI, Kahn RS. Genetic contributions to human brain morphology and intelligence. Journal of Neuroscience. 2006; 26:10235–10242. [PubMed: 17021179]

Jahanshad N, Lee AD, Barysheva M, McMahon KL, de Zubicaray GI, Martin NG, Wright MJ, Toga AW, Thompson PM. Genetic influences on brain asymmetry; A DTI study of 374 twins and siblings. Neuroimage. 2010; 52:455–469. [PubMed: 20430102]

Karlsgodt KH, Kochunov P, Winkler AM, Laird AR, Almasy L, Duggirala R, Olvera RL, Fox PT, Blangero J, Glahn DC. A multimodal assessment of the genetic control over working memory. Journal of Neuroscience. 2010; 30:8197–8202. [PubMed: 20554870]

Kinney HC, Brody BA, Kloman AS, Gilles FH. Sequence of central nervous system myelination in human infancy. II. Patterns of myelination in autopsied infants. Journal of Neuropathology and Experimental Neurology. 1988; 47:217–234. [PubMed: 3367155]

Knickmeyer RC, Gouttard S, Kang C, Evans D, Wilber K, Smith JK, Hamer RM, Lin W, Gerig G, Gilmore JH. A structural MRI study of human brain development from birth to 2 years. Journal of Neuroscience. 2008; 28:12176–12182. [PubMed: 19020011]

Kochunov P, Glahn DC, Lancaster JL, Winkler AM, Smith S, Thompson PM, Almasy L, Duggirala R, Fox PT, Blangero J. Genetics of microstructure of cerebral white matter using diffusion tensor imaging. Neuroimage. 2010; 53:1109–1116. [PubMed: 20117221]

Koten JW Jr, Wood G, Hagoort P, Goebel R, Propping P, Willmes K, Boomsma DI. Genetic contribution to variation in cognitive function: An FMRI study in twins. Science. 2009; 323:1737–1740. [PubMed: 19325117]

Le Bihan D, Mangin JF, Poupon C, Clark CA, Pappata S, Molko N, Chabriat H. Diffusion tensor imaging: Concepts and applications. Journal of Magnetic Resonance Imaging. 2001; 13:534–546. [PubMed: 11276097]

Lenroot RK, Giedd JN. The changing impact of genes and environment on brain development during childhood and adolescence: Initial findings from a neuroimaging study of pediatric twins. Developmental Psychopathology. 2008; 20:1161–1175.

Liu Z, Wang Y, Gerig G, Gouttard S, Tao R, Fletcher T, Styner M. Quality control of diffusion weighted images. Proceedings of SPIE. 2010; 7628:1–9.

Neale, MC.; Cardon, LR. Methodology for genetic studies of twins and families. Dordrecht: Kluwer Academic; 1992.

Neil JJ, Shiran SI, McKinstry RC, Schefft GL, Snyder AZ, Almli CR, Akbudak E, Aronovitz JA, Miller JP, Lee BC, Conturo TE. Normal brain in human newborns: Apparent diffusion coefficient and diffusion anisotropy measured by using diffusion tensor MR imaging. Radiology. 1998; 209:57–66. [PubMed: 9769812]

Oishi K, Faria A, Jiang H, Li X, Akhter K, Zhang J, Hsu JT, Miller MI, van Zijl PC, Albert M, Lyketsos CG, Woods R, Toga AW, Pike GB, Rosa-Neto P, Evans A, Mazziotta J, Mori S. Atlas-based whole brain white matter analysis using large deformation diffeomorphic metric mapping: Application to normal elderly and Alzheimer's disease participants. Neuroimage. 2009; 46:486–499. [PubMed: 19385016]

Panizzon MS, Fennema-Notestine C, Eyler LT, Jernigan TL, Prom-Wormley E, Neale M, Jacobson K, Lyons MJ, Grant MD, Franz CE, Xian H, Tsuang M, Fischl B, Seidman L, Dale A, Kremen WS. Distinct genetic influences on cortical surface area and cortical thickness. Cerebral Cortex. 2009; 19:2728–2735. [PubMed: 19299253]

Partridge SC, Mukherjee P, Henry RG, Miller SP, Berman JI, Jin H, Lu Y, Glenn OA, Ferriero DM, Barkovich AJ, Vigneron DB. Diffusion tensor imaging: Serial quantitation of white matter tract maturity in premature newborns. Neuroimage. 2004; 22:1302–1314. [PubMed: 15219602]

Peper JS, Brouwer RM, Boomsma DI, Kahn RS, Hulshoff Pol HE. Genetic influences on human brain structure: A review of brain imaging studies in twins. Human Brain Mapping. 2007; 28:464–473. [PubMed: 17415783]

Peper JS, Schnack HG, Brouwer RM, Van Baal GC, Pjetri E, Szekely E, van Leeuwen M, van den Berg SM, Collins DL, Evans AC, Boomsma DI, Kahn RS, Hulshoff Pol HE. Heritability of regional and global brain structure at the onset of puberty: A magnetic resonance imaging study in 9-year-old twin pairs. Human Brain Mapping. 2009; 30:2184–2196. [PubMed: 19294640]

Pfefferbaum A, Sullivan EV, Carmelli D. Genetic regulation of regional microstructure of the corpus callosum in late life. Neuroreport. 2001; 12:1677–1681. [PubMed: 11409738]

Posthuma D, de Geus EJ, Neale MC, Hulshoff Pol HE, Baare WEC, Kahn RS, Boomsma D. Multivariate genetic analysis of brain structure in an extended twin design. Behavior Genetics. 2000; 30:311–319. [PubMed: 11206086]

Schmitt JE, Eyler LT, Giedd JN, Kremen WS, Kendler KS, Neale MC. Review of twin and family studies on neuroanatomic phenotypes and typical neurodevelopment. Twin Research and Human Genetics. 2007; 10:683–694. [PubMed: 17903108]

Schmitt JE, Lenroot RK, Wallace GL, Ordaz S, Taylor KN, Kabani N, Greenstein D, Lerch JP, Kendler KS, Neale MC, Giedd JN. Identification of genetically mediated cortical networks: A multivariate study of pediatric twins and siblings. Cerebral Cortex. 2008; 18:1737–1747. [PubMed: 18234689]

Song SK, Sun SW, Ju WK, Lin SJ, Cross AH, Neufeld AH. Diffusion tensor imaging detects and differentiates axon and myelin degeneration in mouse optic nerve after retinal ischemia. Neuroimage. 2003; 20:1714–1722. [PubMed: 14642481]

Song SK, Sun SW, Ramsbottom MJ, Chang C, Russell J, Cross AH. Dysmyelination revealed through MRI as increased radial (but unchanged axial) diffusion of water. Neuroimage. 2002; 17:1429–1436. [PubMed: 12414282]

Thompson PM, Cannon TD, Narr KL, van Erp T, Poutanen VP, Huttunen M, Lonnqvist J, Standertskjold-Nordenstam CG, Kaprio J, Khaledy M, Dail R, Zoumalan CI, Toga AW. Genetic influences on brain structure. Nature Neuroscience. 2001; 4:1253–1258.

Yakovlev, PI.; Lecours, AR. The myelogenetic cycles of regional maturation in the brain. In: Minowski, A., editor. Regional development of the brain in early life. Oxford UK: Blackwell; 1967. p. 3-69.

Zhang H, Avants BB, Yushkevich PA, Woo JH, Wang S, McCluskey LF, Elman LB, Melhem ER, Gee JC. High-dimensional spatial normalization of diffusion tensor images improves the detection of white matter differences: An example study using amyotrophic lateral sclerosis. IEEE Transactions on Medical Imaging. 2007; 26:1585–1597. [PubMed: 18041273]

Appendix

List of Abbreviations of Regions of Interest (ROIs)

A, Angular gyrus

ACR, Anterior corona radiata

ALIC, Anterior limb of internal capsule

BCC, Body of corpus callosum

Cerebel, Cerebellum cortex

CGC, Cingulum (cingulate gyrus)

CGH, Cingulum (hippocampus)

Cing, Cingulate gyrus

CP, Cerebral peduncle

CST, Corticospinal tract

Cu, Cuneus

EC, External capsule

Fu, Fusiform gyrus

Fx/ST, Fornix (cres)/Stria terminalis (cannot be resolved with current resolution)

GCC, Genu of corpus callosum

IF, Inferior frontal gyrus

IFO, Inferior fronto-occipital fasciculus

IO, Inferior occipital gyrus

IT, Inferior temporal gyrus

L, Lingual gyrus

LFO, Lateral fronto-orbital gyrus

MCP, Middle cerebellar peduncle

MF, Middle frontal gyrus

MFO, Middle fronto-orbital gyrus Midbrain

MO, Middle occipital gyrus

MT, Middle temporal gyrus

PCR, Posterior corona radiata

PCT, Pontine crossing tract (a part of MCP)

PLIC, Posterior limb of internal capsule

PoC, Post-central gyrus

PrC, Pre-central gyrus

PrCu, Pre-cuneus

PTR, Posterior thalamic radiation (includes optic radiation)

r peduncle

R, Rectus gyrus

RLIC, Retrolenticular part of internal capsule

SCC, Splenium of corpus callosum

SCP, Superior

SCR, Superior corona radiate

SF, Superior frontal gyrus

SFO, Superior fronto-occipital fasciculus (could be a part of ALIC)

SLF, Superior longitudinal fasciculus

SM, Supramarginal gyrus

SO, Superior occipital gyrus

SP, Superior parietal lobule

SS, Sagittal stratum (includes ILF and IFO)

ST, Superior temporal gyrus

Tap, Tapetum

UF, Uncinate fasciculus

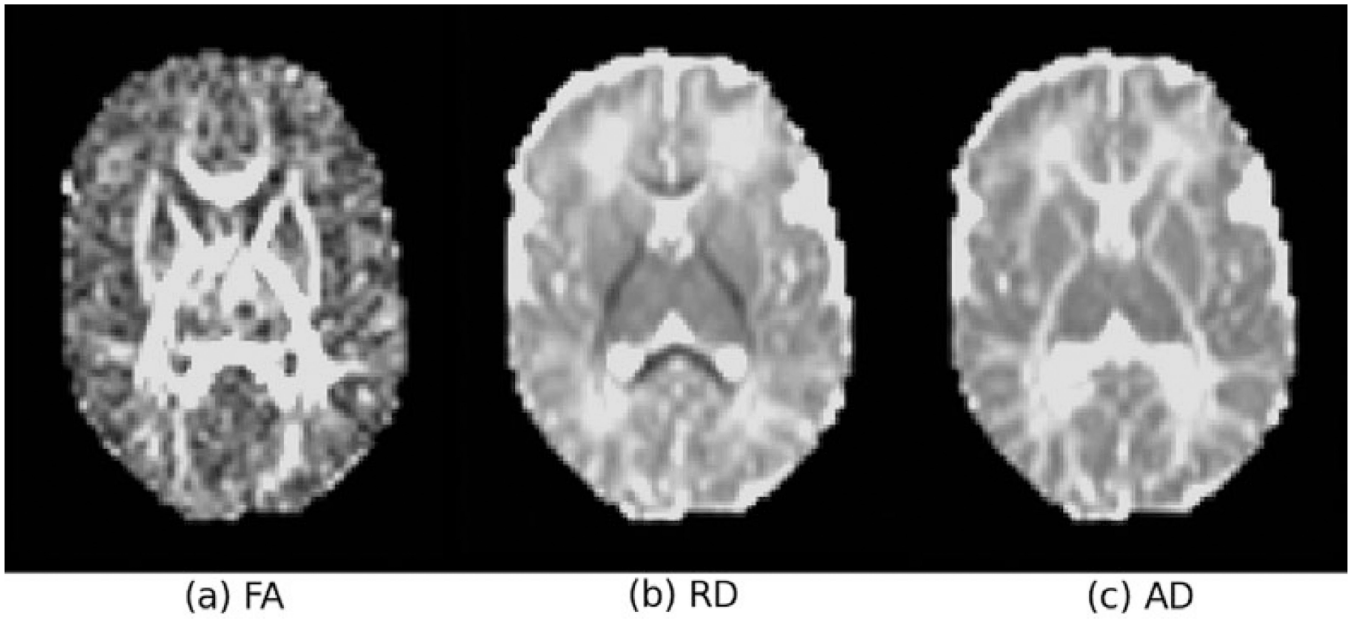

FIGURE 1.
The FA (fractional anisotropy), RD (radial diffusivity) and AD (axial diffusivity) maps of a typical original diffusion tensor imaging (DTI) data.

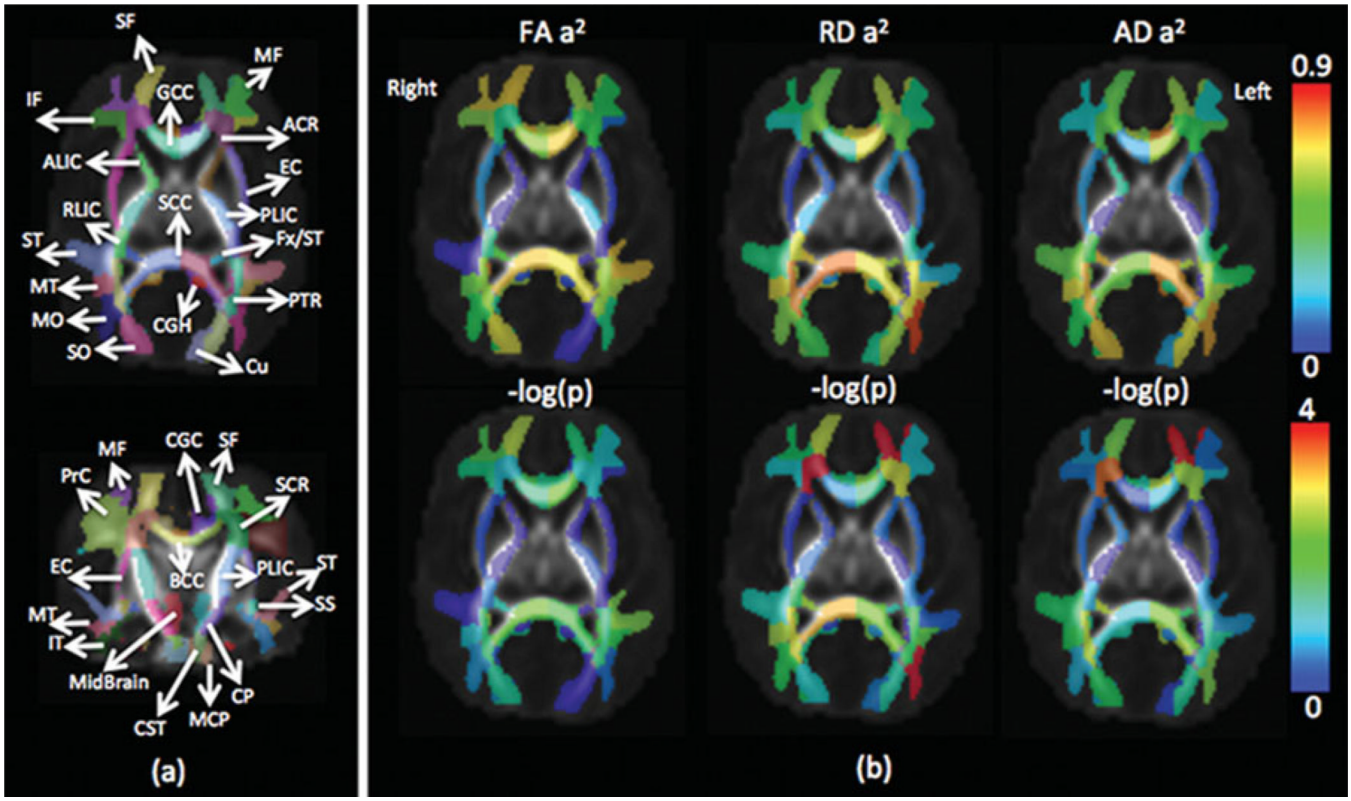

FIGURE 2.

(a) Illustration of white matter regions of interest (ROIs) in the neonatal image space; (b) heritability values of FA, RD and AD over each ROI and their corresponding p values (normalized using −log(p), −log(0.05) = 1.3, and −log(0.0001) = 4). Note: see Appendix for ROI abbreviations; image left corresponds to brain left.

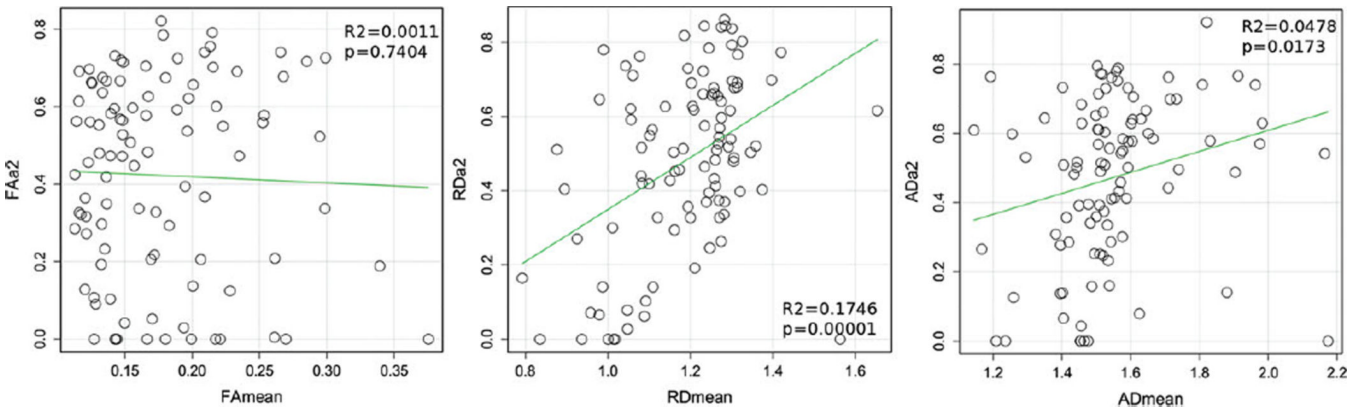

FIGURE 3.
Correlation plots between mean diffusion parameters (RD, AD and FA) and their heritability values over 98 white matter ROIs.

TABLE 1

Demographic Characteristics for Participants

Gender	MZ twins	DZ twins	Single twin	Total
Male (%)	36 (58.1)	34 (53.1)	17 (36.2)	87 (50.3)
Female (%)	26 (41.9)	30 (46.9)	30 (63.8)	86 (49.7)
Ethnicity				
Caucasian (%)	42 (67.7)	38 (59.4)	39 (83.0)	119 (68.8)
African American (%)	14 (22.6)	26 (40.6)	7 (14.9)	47 (27.2)
Other (%)	6 (9.7)	0 (0)	1 (2.1)	7 (4.0)
Mean gestational age (days) at birth (*SD*)	241.9 (20.4)	251.3 (16.1)	247.4 (16.1)	246.8 (18.1)
Mean gestational age (days) at MRI (*SD*)	283.6 (13.4)	291.0 (20.6)	293.5 (24.0)	289.0 (19.8)
Mean birth weight (g) (*SD*)	2168.4 (579.4)	2392.0 (513.2)	2386.7 (470.4)	2310.4 (534.8)

Note: MZ = monozygotic, DZ = dizygotic, *SD* = standard deviation

TABLE 2

Genetic and Common Environmental Contribution Estimates for Whole Brain, Left, and Right Hemisphere White Matter, Diffusion Tensor Imaging Parameters

Measure	Mean	*r*MZ	*r*DZ	a^2 [95% CI]	*p*-value	c^2 [95% CI]	*p*-value
WB- FA	0.16	.86	.70	**.60 [.22, .91]**	**.0021**	.25 (0, .61)	.3402
WB- RD	1.21	.86	.76	**.53 [.19, .91]**	**.0021**	.34 (0, .65)	.1525
WB- AD	1.55	.83	.67	**.57 [.19, .90]**	**.0039**	.27 (0, .62)	.2805
L- FA	0.16	.84	.71	**.56 [.16, .89]**	**.0060**	.28 (0, .64)	.293
L- RD	1.21	.84	.73	**.45 [.09, .88]**	**.0151**	.39 (0, .70)	.1211

Note: a^2 = genetic contribution, c^2 = common environmental contribution, CI = confidenc interval, WB = whole brain, L = left, R = right, MZ = monozygotic, DZ = dizygotic

TABLE 3

Regional Heritability of FA and RD Under Four Conditions: High FA and Low RD; High FA and High RD; Low FA and Low RD; and Low FA and High RD

	High FA			**Low FA**		
Low RD	**ROI (HL)**	**a^2_{RD}**	**a^2_{FA}**	**ROI (LL)**	**a^2_{RD}**	**a^2_{FA}**
	L PLIC	0	.19	L Cerebel	.74*	.66*
	R PLIC	.16	0	R Cerebel	.78*	.70*
	L ALIC	.14	0			
	R ALIC	.07	0			
	L RLIC	.30	0			
	R RLIC	.65*	.34			
	R CP	0	.21			
	R SCP	.62*	.12			
High RD	ROI (HH)	a^2_{RD}	a^2_{FA}	ROI (LH)	a^2_{RD}	a^2_{FA}
	R PTR	.79*	.55*	L A	.40*	.61*
	L BCC	.70*	.69*	R A	.40*	.33
	R BCC	.77*	.74*	R LFO	.48	.32
	L Tap	0	.60*	L MFO	.70*	.11
				R MFO	.69*	.66*

Note: See Appendix for abbreviations of regions of interest (ROIs), a^2 = genetic contribution, L = left, R = right, HL = high-low, HH = high-high, LL = low-low, LH = low-high.

* = $p < .05$.

TABLE 4

(a)

Genetic and Common Environmental Contribution Estimates of Averaged FA Over Superficial and Deep White Matter Regions of Interest

ROI (Left)	FA	Variance (10^{-3})	*r*MZ	*r*DZ	a^2 [95% CI]	*p* of a^2	c^2 [95% CI]	*p* of c^2
S_SP	0.15	0.43	.77	.58	.47 [.00, .85]	.0507	.29 [.00, .68]	.3088
S_Cing	0.15	0.16	.74	.37	.67 [.08, .83]	.0269*	.05 [.00, .54]	.8826
S_SF	0.15	0.52	.76	.59	.57 [.07, .86]	.0249*	.20 [.00, .60]	.4701
S_MF	0.11	0.35	.76	.58	.43 [.00, .82]	.1048	.30 [.00, .70]	.3142
S_IF	0.14	0.42	.62	.55	.10 [.00, .71]	.7308	.49 [.00, .71]	.1181
S_PrC	0.15	0.34	.68	.42	.57 [.00, .83]	.0482*	.15 [.00, .60]	.6010
S_PoC	0.14	0.26	.67	.27	.73 [.29, .85]	.0048*	.00 [.00, .36]	1.0000
S_A	0.12	0.36	.64	.14	.61 [.18, .79]	.0145*	.00 [.00, .29]	1.0000
S_PrCu	0.12	0.18	.48	.15	.46 [.00, .67]	.1514	.00 [.00, .45]	1.0000
S_Cu	0.14	0.24	.38	.37	.00 [.00, .59]	1.0000	.37 [.00, .56]	.2815
S_L	0.13	0.17	.74	.06	.68 [.29, .81]	.0037*	.00 [.00, .31]	1.0000
S_Fu	0.12	0.16	.47	.28	.27 [.00, .62]	.5363	.13 [.00, .54]	.7484
S_SO	0.14	0.37	.61	.57	.00 [.00, .58]	1.0000	.62 [.08, .75]	.0297*
S_IO	0.13	0.32	.43	.28	.48 [.00, .69]	.2125	.00 [.00, .48]	1.0000
S_MO	0.14	0.21	.50	.34	.35 [.00, .69]	.3671	.15 [.00, .58]	.6645
S_ST	0.15	0.24	.66	.24	.72 [.30, .84]	.0038*	.00 [.00, .34]	1.0000
S_IT	0.14	0.25	.67	.63	.00 [.00, .47]	1.0000	.69 [.24, .80]	.0086*
S_MT	0.16	0.49	.65	−0.06	.60 [.19, .76]	.0109*	.00 [.00, .31]	1.0000
S_LFO	0.12	0.30	.52	.50	.13 [.00, .70]	.6998	.42 [.00, .67]	.1644
S_MFO	0.13	0.40	.61	.52	.11 [.00, .71]	.7265	.48 [.00, .70]	.1338
S_SM	0.12	0.34	.60	.14	.56 [.02, .74]	.0420*	.00 [.00, .40]	1.0000
S_R	0.13	0.35	.39	.22	.09 [.00, .55]	.8457	.23 [.00, .50]	.5911
S_Cerebel	0.13	0.19	.70	.24	.66 [.17, .80]	.0139*	.00 [.00, .39]	1.0000
D_CST	0.18	0.37	.38	.34	.00 [.00, .53]	1.0000	.33 [.00, .53]	.2522
D_SCP	0.21	0.37	.43	.33	.37 [.00, .68]	.3733	.10 [.00, .53]	.7656

(a)

Genetic and Common Environmental Contribution Estimates of Averaged FA Over Superficial and Deep White Matter Regions of Interest

ROI (Left)	FA	Variance (10^{-3})	*r*MZ	*r*DZ	a^2 [95% CI]	*p* of a^2	c^2 [95% CI]	*p* of c^2
D_CP	0.25	0.41	.55	.21	.58 [.03, .77]	.0411*	.00 [.00, .36]	.9931
D_ALIC	0.22	0.52	.51	.54	.00 [.00, .58]	1.0000	.49 [.00, .66]	.0605
D_PLIC	0.34	0.47	.54	.50	.19 [.00, .72]	.5649	.38 [.00, .67]	.2213
D_PTR	0.25	0.92	.79	.51	.56 [.07, .86]	.0263*	.21 [.00, .62]	.4750
D_ACR	0.16	0.72	.76	.66	.45 [.00, .83]	.0900	.28 [.00, .69]	.3558
D_SCR	0.19	0.72	.64	.50	.59 [.04, .84]	.0371*	.14 [.00, .57]	.6107
D_PCR	0.18	0.74	.81	.42	.82 [.36, .90]	.0008*	.00 [.00, .43]	1.0000
D_CGC	0.18	0.37	.68	.42	.68 [.10, .81]	.0235*	.00 [.00, .46]	1.0000
D_CGH	0.15	0.39	.57	.56	.04 [.00, .68]	.8920	.52 [.00, .70]	.0827
D_FxST	0.26	0.43	.39	.38	.00 [.00, .60]	.9909	.38 [.00, .57]	.2929
D_SLF	0.17	0.68	.86	.61	.48 [.09, .88]	.0157*	.34 [.00, .69]	.2172
D_SFO	0.19	0.93	.50	.05	.39 [.00, .62]	.1763	.00 [.00, .43]	1.0000
D_IFO	0.20	0.54	.49	.40	.54 [.00, .75]	.1699	.03 [.00, .53]	.9256
D_SS	0.22	0.65	.71	.20	.70 [.32, .84]	.0039*	.00 [.00, .28]	1.0000
D_EC	0.19	0.33	.36	.42	.03 [.00, .63]	.9427	.37 [.00, .58]	.2584
D_UF	0.20	0.47	.63	.01	.62 [.23, .80]	.0090*	.00 [.00, .21]	1.0000
D_PCT	0.20	0.56	.34	.48	.00 [.00, .50]	1.0000	.42 [.00, .60]	.0723
D_MCP	0.20	0.49	.66	.35	.66 [.00, .80]	.0480*	.00 [.00, .53]	1.0000
D_GCC	0.29	1.01	.79	.51	.72 [.19, .87]	.0073*	.06 [.00, .52]	.8504
D_BCC	0.23	0.83	.75	.24	.69 [.24, .82]	.0065*	.00 [.00, .37]	1.0000
D_SCC	0.27	0.68	.79	.45	.68 [.15, .86]	.0124*	.08 [.00, .55]	.7846
D_RLIC	0.27	0.55	.41	.62	.00 [.00, .63]	1.0000	.46 [.00, .63]	.1064
D_Tap	0.22	1.51	.82	.46	.60 [.14, .88]	.0105*	.20 [.00, .61]	.4993
D_Midbrain	0.18	0.24	.57	.48	.29 [.00, .74]	.3824	.28 [.00, .65]	.3497
ROI (Right)	**FA**	**Variance (10−3)**	***r*MZ**	***r*DZ**	**a^2 [95% CI]**	***p* of a^2**	**c^2 [95% CI]**	***p* of c^2**

(a)

Genetic and Common Environmental Contribution Estimates of Averaged FA Over Superficial and Deep White Matter Regions of Interest

ROI (Left)	FA	Variance (10^{-3})	*r*MZ	*r*DZ	a^2 [95% CI]	*p* of a^2	c^2 [95% CI]	*p* of c^2
S_SP	0.13	0.34	.76	.67	.30 [.00, .81]	.1796	.46 [.00, .77]	.0802
S_Cing	0.14	0.06	.67	.15	.60 [.05, .76]	.0342*	.00 [.00, .43]	1.0000
S_SF	0.15	0.52	.86	.60	.72 [.26, .90]	.0020*	.11 [.00, .53]	.6988
S_MF	0.12	0.38	.76	.24	.69 [.25, .82]	.0064*	.00 [.00, .37]	1.0000
S_IF	0.13	0.46	.79	.47	.55 [.05, .85]	.0304*	.21 [.00, .63]	.4887
S_PrC	0.15	0.35	.68	.52	.53 [.04, .86]	.0339*	.24 [.00, .63]	.3781
S_PoC	0.14	0.28	.59	.36	.58 [.00, .79]	.0861	.06 [.00, .56]	.8499
S_A	0.12	0.19	.36	.13	.33 [.00, .57]	.3261	.00 [.00, .42]	1.0000
S_PrCu	0.11	0.27	.32	.08	.28 [.00, .55]	.3766	.00 [.00, .39]	1.0000
S_Cu	0.12	0.24	.43	.17	.32 [.00, .59]	.4966	.05 [.00, .51]	.9088
S_L	0.11	0.13	.52	.34	.56 [.00, .76]	.1360	.02 [.00, .53]	.9501
S_Fu	0.12	0.19	.64	.64	.36 [.00, .78]	.2251	.29 [.00, .67]	.3268
S_SO	0.14	0.30	.61	.47	.67 [.03, .82]	.0408*	.02 [.00, .51]	.9589
S_IO	0.14	0.24	.55	.22	.47 [.00, .67]	.2186	.00 [.00, .53]	1.0000
S_MO	0.14	0.24	.57	.46	.42 [.00, .75]	.2301	.16 [.00, .61]	.6075
S_ST	0.17	0.28	.45	.57	.00 [.00, .65]	1.0000	.55 [.00, .70]	.0603
S_IT	0.14	0.20	.56	.43	.23 [.00, .72]	.4923	.33 [.00, .66]	.3141
S_MT	0.15	0.41	.66	.42	.51 [.00, .79]	.1172	.14 [.00, .62]	.6692
S_LFO	0.12	0.32	.60	.43	.32 [.00, .74]	.3436	.27 [.00, .65]	.3929
S_MFO	0.13	0.27	.72	.30	.66 [.07, .80]	.0306*	.00 [.00, .49]	1.0000
S_SM	0.13	0.30	.49	.44	.19 [.00, .69]	.6058	.30 [.00, .61]	.3503
S_R	0.13	0.15	.33	.71	.00 [.00, .36]	1.0000	.50 [.16, .67]	.0127*
S_Cerebel	0.12	0.18	.66	.37	.70 [.15, .83]	.0176*	.00 [.00, .41]	1.0000
D_CST	0.21	0.67	.32	.28	.21 [.00, .59]	.6496	.12 [.00, .48]	.7313
D_SCP	0.23	0.39	.40	.41	.12 [.00, .67]	.7549	.32 [.00, .59]	.3034
D_CP	0.26	0.46	.19	.04	.21 [.00, .50]	.4849	.00 [.00, .34]	1.0000
D_ALIC	0.22	0.49	.35	.54	.00 [.00, .55]	1.0000	.47 [.00, .64]	.0561

(a)

Genetic and Common Environmental Contribution Estimates of Averaged FA Over Superficial and Deep White Matter Regions of Interest

ROI (Left)	FA	Variance (10^{-3})	*r*MZ	*r*DZ	a^2 [95% CI]	*p* of a^2	c^2 [95% CI]	*p* of c^2
D_PLIC	0.38	0.57	.39	.50	.00 [.00, .63]	1.0000	.50 [.00, .66]	.0794
D_PTR	0.22	0.74	.78	.56	.55 [.08, .87]	.0220*	.23 [.00, .62]	.3993
D_ACR	0.16	0.98	.78	.75	.34 [.00, .83]	.1195	.43 [.00, .76]	.0907
D_SCR	0.19	0.52	.71	.44	.73 [.19, .84]	.0116*	.00 [.00, .44]	1.0000
D_PCR	0.17	0.90	.69	.42	.63 [.02, .83]	.0414*	.07 [.00, .54]	.7943
D_CGC	0.17	0.29	.68	.30	.71 [.26, .83]	.0071*	.00 [.00, .34]	1.0000
D_CGH	0.17	0.31	.20	.24	.05 [.00, .56]	.9114	.22 [.00, .47]	.5347
D_FxST	0.23	0.35	.52	.03	.47 [.00, .69]	.0623	.00 [.00, .36]	1.0000
D_SLF	0.17	0.64	.70	.61	.33 [.00, .81]	.1935	.39 [.00, .73]	.1536
D_SFO	0.13	0.39	.64	.26	.64 [.03, .79]	.0391*	.00 [.00, .47]	1.0000
D_IFO	0.21	0.42	.70	.31	.74 [.38, .86]	.0018*	.00 [.00, .27]	1.0000
D_SS	0.21	0.56	.81	.41	.76 [.25, .86]	.0056*	.00 [.00, .43]	1.0000
D_EC	0.20	0.39	.58	.61	.14 [.00, .73]	.6380	.48 [.00, .72]	.1062
D_UF	0.17	0.24	.57	.23	.58 [.00, .75]	.0535	.00 [.00, .44]	1.0000
D_PCT	0.17	0.59	.46	.44	.21 [.00, .71]	.5761	.31 [.00, .62]	.2992
D_MCP	0.21	0.59	.78	.23	.79 [.52, .89]	.0002**	.00 [.00, .22]	1.0000
D_GCC	0.29	0.76	.73	.58	.52 [.05, .86]	.0321*	.25 [.00, .63]	.3288
D_BCC	0.27	1.04	.74	.39	.74 [.30, .85]	.0035*	.00 [.00, .37]	1.0000
D_SCC	0.30	0.67	.83	.42	.73 [.18, .87]	.0073*	.05 [.00, .55]	.8821
D_RLIC	0.30	0.58	.63	.46	.34 [.00, .75]	.3234	.25 [.00, .63]	.4010
D_Tap	0.18	1.71	.78	.43	.79 [.30, .88]	.0024*	.00 [.00, .43]	1.0000
D_Midbrain	0.17	0.23	.51	.38	.22 [.00, .69]	.5572	.28 [.00, .61]	.3862

(b)

Genetic and Common Environmental Contribution Estimates of Average RD Over Superficial and Deep White Matter Regions of Interest

ROI (Left)	RD	Variance (10^{-3})	*r*MZ	*r*DZ	a^2 [95% CI]	*p* of a^2	c^2 [95% CI]	*p* of c^2
S_SP	1.31	1.52	.87	.67	.49 [.12, .89]	.0097 *	.35 [.00, .68]	.1737
S_Cing	1.20	0.57	.80	.58	.69 [.23, .89]	.0037 *	.12 [.00, .53]	.6538
S_SF	1.30	1.57	.91	.78	.62 [.30, .94]	.0001 **	.30 [.00, .61]	.2203
S_MF	1.28	1.04	.79	.68	.34 [.00, .83]	.1060	.45 [.00, .76]	.0810
S_IF	1.24	0.99	.76	.76	.37 [.00, .84]	.0991	.40 [.00, .73]	.1047
S_PrC	1.16	0.90	.87	.76	.50 [.21, .92]	.0008 *	.39 [.00, .67]	.0834
S_PoC	1.15	0.69	.73	.60	.43 [.00, .85]	.0651	.34 [.00, .70]	.1741
S_A	1.37	1.22	.88	.73	.40 [.14, .81]	.0032 *	.49 [.08, .74]	.0232 *
S_PrCu	1.26	0.91	.81	.53	.68 [.23, .89]	.0035 *	.14 [.00, .53]	.5837
S_Cu	1.20	0.77	.61	.44	.33 [.00, .76]	.3084	.28 [.00, .66]	.3574
S_L	1.30	1.21	.62	−.06	.54 [.04, .72]	.0369 *	.00 [.00, .40]	1.0000
S_Fu	1.27	0.88	.59	.59	.37 [.00, .82]	.1611	.34 [.00, .70]	.1820
S_SO	1.23	0.85	.67	.48	.58 [.00, .83]	.0479 *	.14 [.00, .58]	.6051
S_IO	1.27	1.20	.81	.42	.84 [.53, .91]	.0001 **	.00 [.00, .29]	1.0000
S_MO	1.28	1.05	.84	.45	.86 [.43, .92]	.0001 **	.00 [.00, .41]	1.0000
S_ST	1.21	0.85	.66	.65	.19 [.00, .76]	.4459	.50 [.00, .76]	.0725
S_IT	1.27	0.88	.65	.62	.33 [.00, .80]	.2243	.36 [.00, .71]	.1735
S_MT	1.31	1.38	.80	.53	.68 [.19, .88]	.0066 *	.11 [.00, .55]	.6952
S_LFO	1.27	1.02	.78	.59	.57 [.07, .86]	.0263 *	.19 [.00, .60]	.4802
S_MFO	1.30	1.37	.83	.61	.70 [.28, .91]	.0013 *	.15 [.00, .53]	.5758
S_SM	1.28	1.17	.82	.59	.60 [.19, .90]	.0050 *	.23 [.00, .59]	.3423
S_R	1.25	0.87	.80	.72	.39 [.03, .86]	.0362 *	.43 [.00, .73]	.0718
S_Cerebel	1.04	0.60	.71	.37	.74 [.20, .85]	.0094 *	.00 [.00, .44]	1.0000
D_CST	1.08	0.48	.69	.41	.44 [.00, .79]	.1547	.21 [.00, .66]	.5035
D_SCP	1.06	0.35	.71	.49	.59 [.08, .86]	.0238 *	.17 [.00, .58]	.5190
D_CP	1.08	0.31	.58	.36	.52 [.00, .76]	.1441	.08 [.00, .58]	.7945
D_ALIC	0.99	0.45	.78	.75	.14 [.00, .54]	.3899	.66 [.28, .84]	.0031 *

(b)

Genetic and Common Environmental Contribution Estimates of Average RD Over Superficial and Deep White Matter Regions of Interest

ROI (Left)	RD	Variance (10^{-3})	*r*MZ	*r*DZ	a^2 [95% CI]	*p* of a^2	c^2 [95% CI]	*p* of c^2
D_PLIC	0.83	0.24	.79	.69	.00 [.00, .45]	1.0000	.74 [.31, .83]	.0044 *
D_PTR	1.26	1.60	.74	.11	.66 [.15, .80]	.0154 *	.00 [.00, .45]	1.0000
D_ACR	1.35	2.03	.89	.76	.50 [.19, .91]	.0015 *	.38 [.00, .68]	.1142
D_SCR	1.21	1.99	.91	.69	.63 [.30, .94]	.0000 ***	.28 [.00, .61]	.2622
D_PCR	1.33	2.38	.93	.52	.80 [.42, .96]	.0000 ***	.12 [.00, .51]	.6486
D_CGC	1.19	0.71	.78	.43	.73 [.25, .84]	.0056 *	.00 [.00, .41]	1.0000
D_CGH	1.12	0.36	.70	.52	.33 [.00, .80]	.2103	.37 [.00, .72]	.1873
D_FxST	1.11	0.79	.61	.16	.56 [.00, .74]	.0545	.00 [.00, .46]	1.0000
D_SLF	1.26	1.51	.92	.72	.51 [.23, .93]	.0002 *	.41 [.00, .68]	.0837
D_SFO	1.08	0.93	.72	.40	.76 [.23, .86]	.0066 *	.00 [.00, .46]	.9906
D_IFO	1.10	0.58	.60	.64	.42 [.00, .83]	.1087	.31 [.00, .68]	.1994
D_SS	1.24	1.03	.75	.45	.78 [.33, .88]	.0022 *	.00 [.00, .39]	1.0000
D_EC	1.09	0.61	.78	.85	.10 [.00, .42]	.4503	.73 [.42, .87]	.0003 **
D_UF	1.02	0.19	.45	.57	.00 [.00, .56]	1.0000	.51 [.01, .67]	.0453 *
D_PCT	0.88	0.21	.69	.35	.51 [.00, .79]	.1058	.15 [.00, .64]	.6521
D_MCP	1.09	0.75	.72	.57	.06 [.00, .65]	.7955	.62 [.06, .78]	.0336 *
D_GCC	1.25	1.66	.71	.43	.66 [.06, .83]	.0304 *	.05 [.00, .54]	.8743
D_BCC	1.40	2.13	.73	.31	.70 [.17, .82]	.0127 *	.00 [.00, .43]	1.0000
D_SCC	1.27	1.19	.82	.48	.66 [.18, .88]	.0065 *	.15 [.00, .58]	.6247
D_RLIC	1.01	0.50	.59	.67	.30 [.00, .79]	.2899	.37 [.00, .70]	.1703
D_Tap	1.56	4.44	.60	.49	.00 [.00, .65]	1.0000	.56 [.00, .71]	.0735
D_Midbrain	.96	0.13	.55	.57	.07 [.00, .69]	.8247	.48 [.00, .68]	.0958
ROI (Right)	**RD**	**Variance (10^{-3})**	***r*MZ**	***r*DZ**	**a^2 [95% CI]**	***p* of a^2**	**c^2 [95% CI]**	***p* of c^2**
S_SP	1.27	1.26	.85	.58	.64 [.22, .90]	.0030 *	.19 [.00, .57]	.4672
S_Cing	1.23	0.34	.71	.42	.66 [.05, .82]	.0338 *	.04 [.00, .55]	.9068
S_SF	1.29	1.58	.89	.79	.52 [.19, .91]	.0017 *	.36 [.00, .67]	.1424

(b)

Genetic and Common Environmental Contribution Estimates of Average RD Over Superficial and Deep White Matter Regions of Interest

ROI (Left)	RD	Variance (10^{-3})	*r*MZ	*r*DZ	a^2 [95% CI]	*p* of a^2	c^2 [95% CI]	*p* of c^2
S_MF	1.28	1.02	.86	.77	.37 [.06, .84]	.0214 *	.49 [.02, .75]	.0403 *
S_IF	1.27	1.26	.85	.80	.26 [.00, .70]	.1013	.57 [.14, .82]	.0156 *
S_PrC	1.16	0.87	.86	.79	.45 [.16, .90]	.0027 *	.43 [.00, .70]	.0555
S_PoC	1.14	0.66	.75	.61	.63 [.23, .90]	.0036 *	.21 [.00, .56]	.3759
S_A	1.32	0.94	.82	.66	.40 [.02, .86]	.0374 *	.42 [.00, .73]	.0907
S_PrCu	1.29	1.24	.83	.49	.84 [.39, .91]	.0003 **	.00 [.00, .43]	.9999
S_Cu	1.17	0.74	.78	.64	.46 [.03, .86]	.0370 *	.34 [.00, .68]	.1688
S_L	1.23	0.74	.84	.34	.72 [.14, .85]	.0135 *	.03 [.00, .56]	.9410
S_Fu	1.26	0.86	.49	.59	.43 [.00, .81]	.1559	.25 [.00, .65]	.3306
S_SO	1.23	0.93	.57	.60	.47 [.00, .84]	.0851	.27 [.00, .65]	.2624
S_IO	1.26	0.93	.67	.49	.48 [.00, .81]	.1106	.19 [.00, .63]	.4953
S_MO	1.27	0.92	.79	.63	.54 [.13, .88]	.0115 *	.27 [.00, .62]	.2617
S_ST	1.19	0.76	.78	.70	.36 [.00, .84]	.0650	.45 [.00, .75]	.0570
S_IT	1.30	0.88	.71	.44	.84 [.57, .91]	.0001 **	.00 [.00, .23]	1.0000
S_MT	1.31	1.21	.84	.59	.68 [.25, .90]	.0025 *	.15 [.00, .54]	.5567
S_LFO	1.30	1.41	.86	.65	.48 [.08, .88]	.0201 *	.34 [.00, .68]	.2128
S_MFO	1.31	1.36	.78	.53	.69 [.15, .85]	.0134 *	.06 [.00, .53]	.8395
S_SM	1.26	0.97	.85	.79	.41 [.11, .85]	.0085 *	.46 [.02, .72]	.0401 *
S_R	1.25	0.70	.70	.72	.25 [.00, .78]	.3354	.45 [.00, .74]	.0951
S_Cerebel	.99	0.47	.84	.45	.78 [.33, .91]	.0006 *	.06 [.00, .49]	.8161
D_CST	.93	0.26	.72	.46	.27 [.00, .78]	.3329	.40 [.00, .73]	.2248
D_SCP	1.06	0.40	.58	.34	.62 [.00, .78]	.0517 *	.00 [.00, .46]	1.0000
D_CP	1.01	0.24	.11	.31	.00 [.00, .46]	1.0000	.22 [.00, .44]	.2952
D_ALIC	.98	0.38	.71	.74	.07 [.00, .48]	.7200	.69 [.30, .83]	.0025 *
D_PLIC	.79	0.23	.76	.62	.16 [.00, .69]	.4411	.57 [.06, .80]	.0308 *
D_PTR	1.30	2.34	.82	.33	.79 [.33, .88]	.0014 *	.00 [.00, .43]	1.0000

(b)

Genetic and Common Environmental Contribution Estimates of Average RD Over Superficial and Deep White Matter Regions of Interest

ROI (Left)	RD	Variance (10^{-3})	*r*MZ	*r*DZ	a^2 [95% CI]	*p* of a^2	c^2 [95% CI]	*p* of c^2
D_ACR	1.36	2.29	.93	.75	.50 [.24, .94]	.0001**	.40 [.00, .68]	.0872
D_SCR	1.21	1.60	.90	.71	.62 [.28, .93]	.0002**	.28 [.00, .61]	.2643
D_PCR	1.42	2.83	.94	.58	.77 [.42, .97]	.0000***	.17 [.00, .53]	.4981
D_CGC	1.18	0.52	.78	.62	.51 [.07, .87]	.0229*	.28 [.00, .65]	.2844
D_CGH	1.11	0.28	.52	.50	.14 [.00, .70]	.6795	.39 [.00, .66]	.1910
D_FxST	1.06	0.58	.70	.01	.71 [.36, .86]	.0028*	.00 [.00, .16]	1.0000
D_SLF	1.27	1.66	.91	.76	.53 [.25, .94]	.0001**	.39 [.00, .67]	.0830
D_SFO	1.10	0.66	.65	.52	.55 [.00, .82]	.0718	.14 [.00, .60]	.6323
D_IFO	1.08	0.53	.72	.64	.42 [.00, .86]	.0521	.37 [.00, .70]	.1165
D_SS	1.23	1.05	.76	.24	.84 [.64, .92]	.0001**	.00 [.00, .16]	1.0000
D_EC	1.05	0.58	.82	.87	.03 [.00, .29]	.8060	.82 [.58, .90]	.0000***
D_UF	1.00	0.16	.71	.70	.00 [.00, .41]	1.0000	.69 [.30, .80]	.0038*
D_PCT	.89	0.25	.75	.45	.40 [.00, .82]	.1218	.32 [.00, .72]	.3019
D_MCP	1.05	0.61	.65	.45	.08 [.00, .70]	.7969	.51 [.00, .72]	.1332
D_GCC	1.16	0.87	.62	.61	.29 [.00, .79]	.2856	.38 [.00, .71]	.1491
D_BCC	1.32	2.00	.75	.41	.77 [.29, .87]	.0035*	.00 [.00, .41]	1.0000
D_SCC	1.19	0.96	.83	.50	.82 [.39, .89]	.0005**	.00 [.00, .40]	1.0000
D_RLIC	.98	0.45	.71	.60	.65 [.12, .86]	.0182*	.11 [.00, .53]	.6695
D_Tap	1.65	5.72	.83	.52	.62 [.18, .89]	.0054*	.20 [.00, .59]	.4611
D_Midbrain	.94	0.09	.51	.41	.00 [.00, .60]	1.0000	.46 [.00, .63]	.1594

(c)

Genetic and Common Environmental Contribution Estimates of Average AD Over Superficial and Deep White Matter Regions of Interest

ROI (Left)	AD	Variance (10^{-3})	*r*MZ	*r*DZ	a^2 [95% CI]	*p* of a^2	c^2 [95% CI]	*p* of c^2
S_SP	1.63	1.18	.80	.46	.64 [.10, .85]	.0195*	.11 [.00, .56]	.7195
S_Cing	1.50	0.46	.77	.48	.79 [.30, .88]	.0023*	.00 [.00, .44]	1.0000
S_SF	1.59	1.03	.91	.78	.58 [.27, .94]	.0001**	.33 [.00, .64]	.1657

Twin Res Hum Genet. Author manuscript; available in PMC 2013 January 21.

(c)

Genetic and Common Environmental Contribution Estimates of Average AD Over Superficial and Deep White Matter Regions of Interest

ROI (Left)	AD	Variance (10^{-3})	*r*MZ	*r*DZ	a^2 [95% CI]	*p* of a^2	c^2 [95% CI]	*p* of c^2
S_MF	1.51	0.66	.65	.59	.25 [.00, .77]	.3544	.42 [.00, .72]	.1270
S_IF	1.51	0.69	.63	.61	.49 [.00, .80]	.1252	.17 [.00, .61]	.5356
S_PrC	1.44	0.66	.81	.75	.52 [.17, .90]	.0049*	.34 [.00, .65]	.1510
S_PoC	1.42	0.53	.66	.60	.29 [.00, .79]	.2684	.41 [.00, .73]	.1154
S_A	1.63	0.92	.78	.75	.08 [.00, .46]	.6330	.71 [.35, .85]	.0014*
S_PrCu	1.51	0.90	.75	.45	.77 [.28, .88]	.0033*	.02 [.00, .45]	.9341
S_Cu	1.49	0.89	.47	.36	.16 [.00, .66]	.6830	.30 [.00, .60]	.3902
S_L	1.59	1.40	.50	−.12	.41 [.00, .63]	.0801	.00 [.00, .37]	1.0000
S_Fu	1.51	0.90	.50	.42	.51 [.00, .79]	.1354	.12 [.00, .58]	.6732
S_SO	1.52	0.88	.65	.34	.66 [.04, .80]	.0384*	.00 [.00, .48]	1.0000
S_IO	1.54	1.15	.73	.33	.76 [.35, .86]	.0021*	.00 [.00, .35]	1.0000
S_MO	1.56	1.04	.76	.32	.75 [.30, .86]	.0036*	.00 [.00, .38]	1.0000
S_ST	1.51	0.72	.62	.56	.39 [.00, .78]	.2183	.24 [.00, .65]	.4333
S_IT	1.58	0.75	.53	.50	.30 [.00, .75]	.3732	.28 [.00, .64]	.3340
S_MT	1.67	1.05	.75	.50	.58 [.02, .83]	.0427	.13 [.00, .59]	.6511
S_LFO	1.51	0.75	.73	.49	.61 [.03, .83]	.0389	.10 [.00, .56]	.7301
S_MFO	1.57	1.02	.59	.52	.46 [.00, .79]	.1602	.18 [.00, .62]	.5350
S_SM	1.52	0.93	.72	.62	.37 [.00, .83]	.1056	.39 [.00, .72]	.1105
S_R	1.50	0.71	.60	.41	.65 [.00, .80]	.0566	.00 [.00, .50]	1.0000
S_Cerebel	1.26	0.55	.66	.46	.60 [.00, .82]	.0532	.09 [.00, .57]	.7582
D_CST	1.40	0.60	.59	.55	.07 [.00, .69]	.8267	.52 [.00, .71]	.0787*
D_SCP	1.44	0.41	.60	.41	.48 [.00, .78]	.1441	.15 [.00, .61]	.6225
D_CP	1.60	0.39	.52	.33	.58 [.00, .76]	.1196	.01 [.00, .54]	.9704
D_ALIC	1.40	0.35	.68	.51	.14 [.00, .72]	.6453	.47 [.00, .71]	.1210
D_PLIC	1.45	0.20	.59	.38	.00 [.00, .61]	1.0000	.51 [.00, .67]	.1107
D_PTR	1.83	1.46	.67	−.01	.58 [.03, .74]	.0394*	.00 [.00, .47]	1.0000
D_ACR	1.71	1.51	.87	.74	.44 [.15, .90]	.0030*	.44 [.00, .71]	.0539
D_SCR	1.60	1.61	.90	.61	.63 [.27, .93]	.0002**	.26 [.00, .61]	.3366

Twin Res Hum Genet. Author manuscript; available in PMC 2013 January 21.

(c)

Genetic and Common Environmental Contribution Estimates of Average AD Over Superficial and Deep White Matter Regions of Interest

ROI (Left)	AD	Variance (10^{-3})	*r*MZ	*r*DZ	a^2 [95% CI]	*p* of a^2	c^2 [95% CI]	*p* of c^2
D_PCR	1.73	2.06	.91	.55	.70 [.32, .93]	.0001**	.19 [.00, .57]	.4825
D_CGC	1.56	0.61	.80	.39	.79 [.33, .88]	.0017*	.00 [.00, .41]	1.0000
D_CGH	1.41	0.30	.54	.36	.36 [.00, .75]	.2981	.23 [.00, .64]	.4717
D_FxST	1.65	0.77	.67	.07	.60 [.13, .76]	.0190*	.00 [.00, .37]	1.0000
D_SLF	1.58	1.02	.88	.66	.55 [.23, .92]	.0008*	.34 [.00, .64]	.1584
D_SFO	1.46	0.87	.77	.26	.68 [.12, .81]	.0194*	.00 [.00, .47]	1.0000
D_IFO	1.48	0.41	.81	.69	.39 [.08, .84]	.0143*	.47 [.03, .73]	.0391*
D_SS	1.71	0.66	.66	.37	.70 [.13, .83]	.0194*	.00 [.00, .45]	1.0000
D_EC	1.46	0.53	.69	.80	.04 [.00, .45]	.8128	.71 [.33, .83]	.0016*
D_UF	1.40	0.23	.21	.13	.28 [.00, .57]	.4860	.00 [.00, .38]	1.0000
D_PCT	1.17	0.20	.76	.41	.27 [.00, .77]	.3551	.40 [.00, .74]	.2620
D_MCP	1.46	0.63	.74	.66	.00 [.00, .47]	1.0000	.70 [.25, .81]	.0071*
D_GCC	1.98	1.41	.62	.28	.57 [.00, .74]	.1253	.01 [.00, .56]	.9848
D_BCC	1.98	2.15	.64	.28	.63 [.03, .78]	.0413*	.00 [.00, .47]	1.0000
D_SCC	1.91	0.91	.80	.34	.77 [.21, .86]	.0063*	.00 [.00, .51]	.9974
D_RLIC	1.53	0.41	.63	.51	.33 [.00, .80]	.2239	.35 [.00, .71]	.2082
D_Tap	2.17	3.67	.42	.35	.00 [.00, .60]	1.0000	.38 [.00, .57]	.2879
D_Midbrain	1.26	0.09	.48	.40	.13 [.00, .68]	.7350	.35 [.00, .62]	.2788
ROI (Right)	**AD**	**Variance (10^{-3})**	***r*MZ**	***r*DZ**	**a^2 [95% CI]**	***p* of a^2**	**c^2 [95% CI]**	***p* of c^2**
S_SP	1.56	1.01	.78	.41	.78 [.32, .87]	.0024*	.00 [.00, .40]	1.0000
S_Cing	1.54	0.34	.71	.48	.56 [.00, .83]	.0528*	.16 [.00, .62]	.6139
S_SF	1.59	1.04	.86	.75	.50 [.15, .90]	.0047*	.36 [.00, .67]	.1515
S_MF	1.52	0.62	.81	.73	.25 [.00, .72]	.1863	.55 [.09, .80]	.0236*
S_IF	1.53	0.83	.76	.72	.23 [.00, .78]	.3293	.48 [.00, .76]	.0715
S_PrC	1.45	0.59	.81	.80	.39 [.02, .86]	.0373*	.43 [.00, .73]	.0686
S_PoC	1.40	0.55	.69	.54	.73 [.26, .89]	.0042*	.07 [.00, .47]	.7673

Twin Res Hum Genet. Author manuscript; available in PMC 2013 January 21.

(c)

Genetic and Common Environmental Contribution Estimates of Average AD Over Superficial and Deep White Matter Regions of Interest

ROI (Left)	AD	Variance (10^{-3})	*r*MZ	*r*DZ	a^2 [95% CI]	*p* of a^2	c^2 [95% CI]	*p* of c^2
S_A	1.57	0.82	.80	.56	.54 [.11, .88]	.0149 *	.26 [.00, .63]	.3178
S_PrCu	1.52	1.12	.76	.39	.77 [.27, .87]	.0041 *	.00 [.00, .44]	1.0000
S_Cu	1.40	0.88	.62	.46	.51 [.00, .80]	.1149	.15 [.00, .60]	.5861
S_L	1.46	0.87	.74	.14	.63 [.07, .77]	.0292 *	.00 [.00, .47]	1.0000
S_Fu	1.50	0.78	.40	.53	.36 [.00, .79]	.2774	.27 [.00, .64]	.2968
S_SO	1.51	0.97	.60	.45	.71 [.15, .86]	.0169 *	.03 [.00, .46]	.8963
S_IO	1.54	0.83	.54	.50	.29 [.00, .76]	.3771	.32 [.00, .66]	.2561
S_MO	1.54	0.81	.64	.51	.41 [.00, .81]	.1601	.27 [.00, .67]	.3218
S_ST	1.53	0.57	.78	.62	.51 [.09, .87]	.0198 *	.30 [.00, .65]	.2365
S_IT	1.59	0.80	.65	.23	.73 [.39, .86]	.0025 *	.00 [.00, .22]	1.0000
S_MT	1.64	0.90	.77	.49	.67 [.14, .86]	.0139 *	.09 [.00, .54]	.7431
S_LFO	1.55	1.11	.79	.59	.41 [.00, .83]	.1081	.31 [.00, .71]	.2834
S_MFO	1.58	1.20	.67	.51	.58 [.00, .80]	.0703	.08 [.00, .58]	.8005
S_SM	1.53	0.74	.79	.63	.60 [.18, .89]	.0071 *	.21 [.00, .58]	.3878
S_R	1.49	0.64	.62	.55	.25 [.00, .73]	.4529	.31 [.00, .65]	.3034
S_Cerebel	1.19	0.41	.82	.45	.76 [.27, .89]	.0024 *	.04 [.00, .49]	.8844
D_CST	1.24	0.27	.44	.45	.00 [.00, .52]	1.0000	.44 [.00, .62]	.0753
D_SCP	1.51	0.45	.48	.24	.57 [.00, .76]	.0531	.00 [.00, .37]	1.0000
D_CP	1.54	0.19	.22	.14	.16 [.00, .49]	.7418	.05 [.00, .40]	.8872
D_ALIC	1.38	0.28	.70	.45	.31 [.00, .77]	.3003	.34 [.00, .71]	.3005
D_PLIC	1.48	0.19	.59	.39	.00 [.00, .65]	1.0000	.53 [.00, .69]	.1199
D_PTR	1.81	2.28	.78	.18	.74 [.32, .85]	.0023 *	.00 [.00, .36]	1.0000
D_ACR	1.74	1.50	.92	.70	.50 [.22, .93]	.0002 **	.42 [.00, .69]	.0845
D_SCR	1.61	1.46	.87	.62	.71 [.31, .92]	.0004 **	.16 [.00, .55]	.5437
D_PCR	1.82	2.41	.93	.46	.92 [.52, .95]	.0000 ***	.00 [.00, .40]	1.0000
D_CGC	1.50	0.54	.71	.47	.61 [.08, .85]	.0262 *	.13 [.00, .56]	.6275
D_CGH	1.44	0.24	.71	.52	.50 [.00, .85]	.0504	.25 [.00, .64]	.3480

(c)

Genetic and Common Environmental Contribution Estimates of Average AD Over Superficial and Deep White Matter Regions of Interest

ROI (Left)	AD	Variance (10^{-3})	*r*MZ	*r*DZ	a^2 [95% CI]	*p* of a^2	c^2 [95% CI]	*p* of c^2
D_FxST	1.53	0.50	.68	.19	.73 [.40, .86]	.0020 *	.00 [.00, .20]	1.0000
D_SLF	1.61	1.30	.91	.69	.64 [.32, .95]	.0000 ***	.28 [.00, .60]	.2363
D_SFO	1.35	0.67	.75	.48	.64 [.11, .85]	.0187 *	.11 [.00, .55]	.7131
D_IFO	1.48	0.42	.80	.74	.34 [.02, .78]	.0392 *	.50 [.08, .77]	.0251 *
D_SS	1.71	0.78	.74	.03	.76 [.48, .88]	.0005 **	.00 [.00, .16]	1.0000
D_EC	1.40	0.47	.81	.76	.14 [.00, .54]	.4040	.66 [.27, .84]	.0036 *
D_UF	1.29	0.18	.53	.25	.53 [.00, .73]	.1011	.00 [.00, .45]	1.0000
D_PCT	1.14	0.14	.72	.29	.61 [.00, .80]	.0653	.06 [.00, .61]	.8752
D_MCP	1.45	0.63	.58	.58	.00 [.00, .39]	1.0000	.58 [.18, .72]	.0157 *
D_GCC	1.88	0.65	.56	.57	.14 [.00, .72]	.6441	.46 [.00, .70]	.1029
D_BCC	1.96	1.64	.70	.29	.74 [.33, .86]	.0034 *	.00 [.00, .32]	1.0000
D_SCC	1.90	0.66	.68	.53	.49 [.00, .81]	.0955	.20 [.00, .65]	.4868
D_RLIC	1.57	0.32	.61	.51	.43 [.00, .79]	.1708	.22 [.00, .64]	.4350
D_Tap	2.16	3.76	.76	.46	.54 [.02, .84]	.0397 *	.20 [.00, .63]	.4904
D_Midbrain	1.21	0.08	.42	.57	.00 [.00, .48]	1.0000	.49 [.03, .65]	.0392 *

Note: See Appendix for abbreviations of regions of interest (ROIs); FA = fractional anisotropy, RD = radial diffusivity, AD = axial diffusivity, a^2 = genetic contribution, c^2 = common environmental contribution, MZ = monozygotic, DZ = dizygotic, CI = confidence interval, S = superficial white matter, D = deep white matter. The unit of RD and AD traits is $10^{-3}mm^2s^{-1}$; other measures are unitless; genetic or environmental effects with $p \leq .0005$ are highlighted.

* = $.0005 < p \leq .05$,

** = $.00001 < p \leq .0005$,

*** $p \leq .00001$.